Application of a Single Area Array Detector for Acquisition, Tracking and Point-Ahead in Space Optical Communications

D. L. Clark, M. Cosgrove, R. VanVranken
Advanced Technology Products
Eastman Kodak Company
Rochester, New York 14653

H. Park, M. Fitzmaurice
NASA Goddard Space Flight Center
Greenbelt, Maryland 20771

Abstract

A study has been made to combine the functions of acquisition, tracking, and point-ahead in space optical communications into a single system utilising an area array detector. This paper presents an analysis of the feasibility of the concept.

The key parameters are: (1) optical power less than 1 pW at 0.86 μm, (2) acquisition in less than 30 seconds in an acquisition field of view (FOV) of 1 mrad, (3) tracking with 0.5 μrad rms noise at 1000 Hz update rate, and (4) point ahead transfer function precision of 0.25 μrad over a region of 150 μrad. Currently available array detectors have been examined. The most demanding specifications are low output noise, a high detection efficiency, a large number of pixels, and frame rates over 1 kHz. A proof-of-concept (POC) demonstration system is currently being built utilising the Kodak HS-40 detector (a 128x128 photodiode array with a 64 channel CCD readout architecture which can be operated at frame rates as high as 40,000/sec). The POC system implements a windowing scheme and special purpose digital signal processing electronics for matched filter acquisition and tracking algorithms.

1 Introduction

Many of the advantages of space-based optical communications systems are the result of the highly collimated beam obtainable with modest size telescopes. Optical systems typically operate with near diffraction limited beam divergence angles of about 5 μrad which yields very large forward gain so that transmitter power can be much lower and the link is less susceptible to intercept and jamming. The small beam divergence is also the source of two major problems: acquisition and tracking of the laser beam. The tracking system must be capable of tracking to about 0.5 μrad with update rates that exceed the highest platform vibration frequency that could induce pointing errors of a fraction of a microradian. Reliable and rapid acquisition is also a difficult problem. The open loop pointing error is typically about 1 mrad or larger which is more than three orders of magnitude larger than the acceptable tracking error. Some systems require rapid acquisition. For example, GEO-LEO links which are broken and restablished on each orbital pass, and GEO-LEO or LEO-aircraft links that need to be switched among several platforms require acquisition within a few seconds.

In order for optical communications to successfully compete with RF and microwave systems, comparable reliability, speed, and simplicity of acquisition and tracking is highly desirable.

1.1 Objectives of the POCAAD Project

The objective of the Proof-of-Concept Area Array Detector (POCAAD) project is to determine the critical parameters, examine alternate approaches, and construct and evaluate a laboratory model of a system that uses an area array detector system to combine three functions into a single system:

- Beacon acquisition
- Beacon tracking
- Point-ahead compensation due to relative motion.

These functions typically are separate functions that involve complex optical systems with multiple beam paths, variable FOV, and complicated scanning algorithms over the acquisition FOV.

Table 1 is a summary of the specifications established by NASA for the proof-of-concept (POC) system. These specifications are the basis for the analysis and design of the POC system.

SYSTEM SPECIFICATIONS	
Optics Specifications	
Aperture Diameter	20 cm
Filter Width	10 Å
Filter Transmittance	0.5
Signal Specifications	
Wavelength	0.86 μm
Power Incident	$\leq 1.0 \times 10^{-12}$ Watts
On Focal Plane	
Background Scene	Earth, Moon, Stars
FOV, Accuracy and Noise Specifications	
Acquisition FOV	1000 μrad
Point Ahead Range	150 μrad
Point Ahead Accuracy	0.25 μrad
Tracking NEA	0.5 μrad rms
Rate Specifications	
Acquisition Time	< 30 sec
Tracking Rate	1-5 kHs

Table 1: System specifications.

Low noise area array detectors that cover the acquisition FOV permit a combined acquisition, tracking, and point-ahead (ATP) staring system that is much simpler, faster, and more reliable. The receiver FOV and the beacon laser beams cover the acquisition FOV which is typically about 1 mrad. The beacon beams are acquired by electronically searching the array sensor FOV. When the beacon has been acquired, the system steers the telescope to nominally center the received beacon beam and enters the tracking mode. The tracking mode must be able to track the position of the beacon to within a small fraction of the transmitted beam divergence angle (typically about 5 μrad) so that tracking is required to about 0.5 μrad, which corresponds to about 1/2000 of the FOV.

The sensitivity of the acquisition detector is critical since it is important that the beacon laser beam fill the acquisition FOV. The signal strength for GEO-GEO or GEO-LEO links with a beacon laser of approximately 1 watt filling a 1 mrad acquisition FOV is in the range of a few hundred to a few thousand photoelectrons. The signal strength is very weak at these power levels and the minimum signal to noise ratio (SNR) is a difficult requirement to meet with array detectors. If the acquisition detector is not sufficiently sensitive the beacon laser must be restricted to a smaller divergence angle and a scanning mode of acquisiton must be adopted.

1.2 Update Rates

The update rates are determined by the disturbances of the line of sight of the system. Platform vibrations will set the upper limit on the update rate. The exact requirements are not easy to predict, but sources such as momentum wheels create disturbances that are on the order of a microradian at frequencies in the range of hundreds of Hs. This implies update rates of several hundred Hs or more may be required with even higher update rate requirements for manuevering platforms or platforms that have other agile components.

1.3 Point-Ahead Correction

In order to correctly point the transmitted laser beam, the relative motion of the platforms must be compensated. The correction is,

$$\Theta_{PA} = 2\left(\frac{v_{rel}}{c}\right) \quad (1)$$

where v_{rel} is the component of the relative velocity that is perpendicular to the line of sight. For orbital velocities of satellites in geosynchronous and low-Earth orbit, the point ahead angle is $\approx \pm 75$ μrad. This is about 15% of the acquisition FOV. The point-ahead angle needs to be precisely set so that it is not a significant contributer to the system pointing error budget. A value of about half the tracking noise equivalent angle (NEA) meets that criteria, and implies point-ahead precision of ≈ 0.25 μrad.

2 System Concept

Figure 1 shows a conceptual block diagram for optical communications acquisition, tracking, and point ahead using an area array detector. This diagram does not include many other components required for functions such as transmit and receive isolation, redundant lasers, etc. The telescope has a gimballed Coudé mount which gives it two independent axes for directing the beam while the position of the transmitter and receiver beams on the optical bench remain fixed. The gimballed telescope provides the slow, large angle beam pointing. The FOV of the system is about 1000 μrad. There are also fine beam steering elements that are capable of small deflections of the incoming beacon beam and the outgoing laser beam within the FOV of the telescope. One fine beam steering element must also provide the rapid steering required for tracking in the presence of disturbances of the line of sight of the system due to platform vibrations. The incoming beacon beam is directed by a beamsplitter (dichroic or polarising) onto the

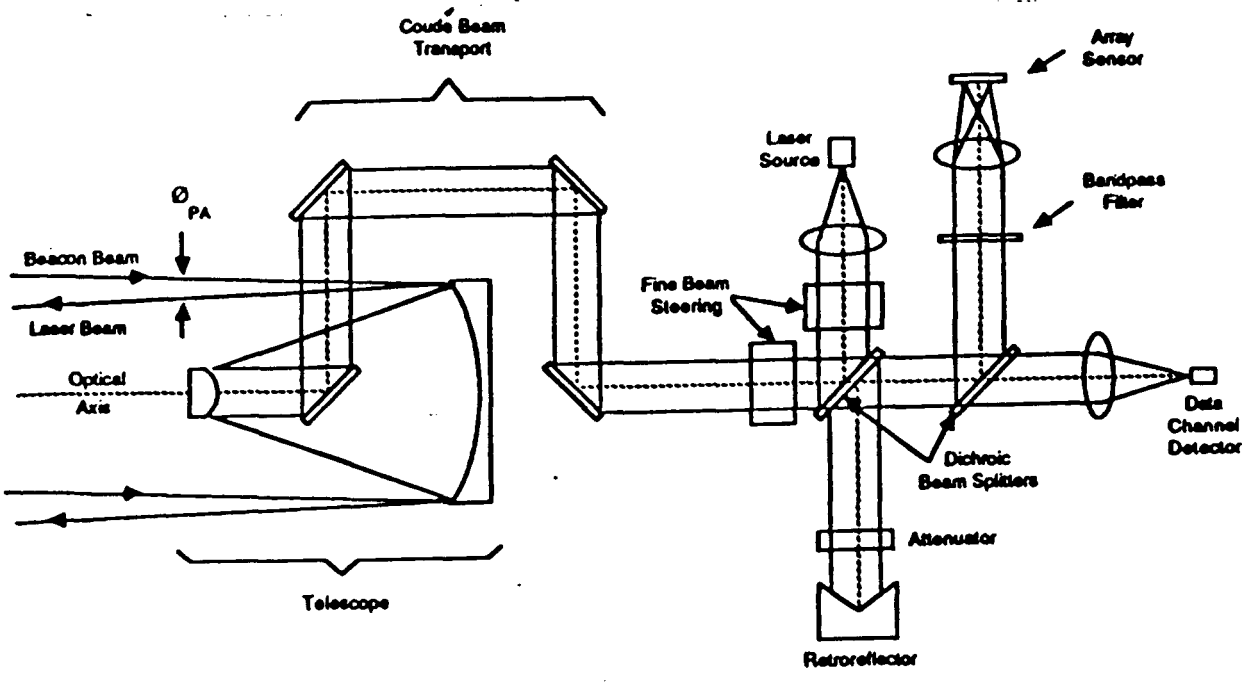

Figure 1: Optical Communications Point-Ahead and Tracking System Concept.

array sensor. An image forming system provides the correct point spread function (PSF) for optimum acquisition and tracking.

The outgoing laser beam, which is the high speed data link, also passes through a fine beam steering element and the gimballed telescope. A tiny fraction of the outgoing beam is back reflected into the the sensor system to provide a reference beam. The reference beam is offset to avoid interference with the beacon beam. The reference beam monitors any instability in the pointing of the laser or instabilities in the components of the optical system not common to the outgoing beam and the incoming beacon.

3 Point-Ahead Compensation

In the concept system shown in Figure 1 there are two fine steering elements; one to direct the laser beam and set the point-ahead angle, the second to stablise the incoming beacon beam on the array sensor and the data beam on the data channel detector. This concept fixes the position of the beacon beam. The reference beam from the outgoing laser moves to indicate the point-ahead angle.

The two spots on the array detector would operate two control loops. The spot due to the reference beam would control the laser beam steerer. The spot due to the incoming beacon would control the beam steerer in the beam adjacent to the telescope. That beam steerer controls both the incoming beacon and data beams and the outgoing laser beam. The control loop to the laser beam steerer can be a relatively slow loop. It needs only to respond to changes in the point-ahead angle as the relative position and velocity of the satellites change. The loop can filter the updates from the array sensor to remove noise. The main beam steerer and control loop must respond at the full update rate to remove beam instabilities in both outgoing and incoming beams.

This configuration has two major advantages:

- The data channel beam is fixed.
- The incoming beacon beam is fixed on the array detector so that the position can be selected to improve tracking performance.

The first advantage is crucial to operation of the data channel. The second can also have a very beneficial impact on the tracking performance of the system.

Use of the reference beam is not necessary. If the stability of the system is such that monitoring the outgoing beam is not necessary, the processor can in effect use a fixed reference that is not monitored and is invariant. The retroreflector components and the sensor and signal processing components required for the reference beam can be removed.

3.1 Point-Ahead Calibration and Tracking

The point-ahead angle precision depends on two operations: calibration of the transfer function of the sensor and the residual systematic error in the tracking algorithm after nonlinearity corrections have been made. The calibration of the system to precision of 0.25 μrad is not a trivial task, but with modern calibration technology, such precision can be attained. Due to the discrete nature of the sampling of the PSF of the beacon image, there are nonlinearities in the computed transfer function which need to be corrected to yield a precise value for the angle. If the sampling, the algorithm, and the nonlinear correction are not adequate, the resultant precision will not meet the pointing accuracy specification. The results of our analysis are presented in Section 6

Acquisition and False Alarm Probability		
Signal Strength (photoelectrons)	Acquisition Probability	False Alarm Probability
796	1.000	0.0000
600	1.000	0.0000
500	0.917	0.0042
400	0.663	0.0042
350	0.488	0.0042
300	0.279	0.0042
250	0.108	0.0083
200	0.021	0.0083
0 †	0.000	0.0042

Table 2: Acquisition and false alarm probability per frame as a function of signal strength. Number of simulated acquisition cycles was 240 (†2400)

4 Background Analysis

Methods to discriminate against stars, planets, Moon, and Earth backgrounds have been analysed. We have found simple methods to discriminate against all of these sources. If the beacon signal collected by a 20 cm aperture is more than 0.1 pW, only the brightest stars rival the in-band signal strength of the beacon and the probability of any being in the FOV is less than one in a million. Even if a bright star were to be in the FOV, either the motion of the star or the broadband spectral distribution of the star makes it easy to identify (e.g. tilting the band pass filter will have little effect on a star, but will cause an incoming laser beam to disappear). The Earth, Moon, and planets are not bright enough in-band to present significant discrimination problems. Again they will move on the wrong trajectory and are broadband sources that are easily identified if they appear in the FOV.

5 Acquisition Analysis

Analysis of the acquisition and tracking of beacons by area array detectors was accomplished with a simulation program ACQTRK that has been developed over a period of two years. The program simulates signals and noise (both random and pattern) in the detectors and the entire signal processing chain including a variety of signal processing algorithms. The beacon sources, including their movement due to orbital dynamics, and star and patterned Earth backgrounds (e.g. clouds) can be simulated.

This program was used to evaluate acquisition performance of a system based on the HS-40 detector (see Section 7.2) and a matched filter acquisition algorithm. The algorithm consists of an optimised 4x4 matched filter that scans the FOV. The matched filter enhances the SNR of the beacon over random noise and patterned background sources that are not the correct size. The output of the matched filter is sent to a peak detector. After the entire frame has been scanned the peak detector indicates the position of the pixel with the largest signal.

Table 2 shows the results of 240 trial acquisitions as a function of signal strength. 250 photoelectrons corresponds to a signal strength of 0.13 pW. It is seen that the acquisition probability is essentially 100% in a single acquisition cycle at powers of 0.3 pW or more. A single acquistion cycle requires only 32 msec. The false alarm rate is very small, only 1 or 2 false acquisitions out of the 240 cases even at the lowest beacon signal strengths. At a power of 0.13 pW beacon power (8x lower than the system specification) there is a probability of 0.96 of beacon acquisition within 4 seconds.

The effectiveness of the matched filter against false acquisition of bright clouds on the surface of the earth has been examined as a function of its size. The conclusion is that the signal is too weak from even the brightest cloud to present any significant acquisition problem. False alarms due to stars in the FOV is extremely unlikely due to the limited number of stars of sufficient brightness to compete with a beacon of only 0.1 pW or more.

6 Tracking Analysis

Determining the precise position of an object in the FOV of a array detector is complicated for point objects due to

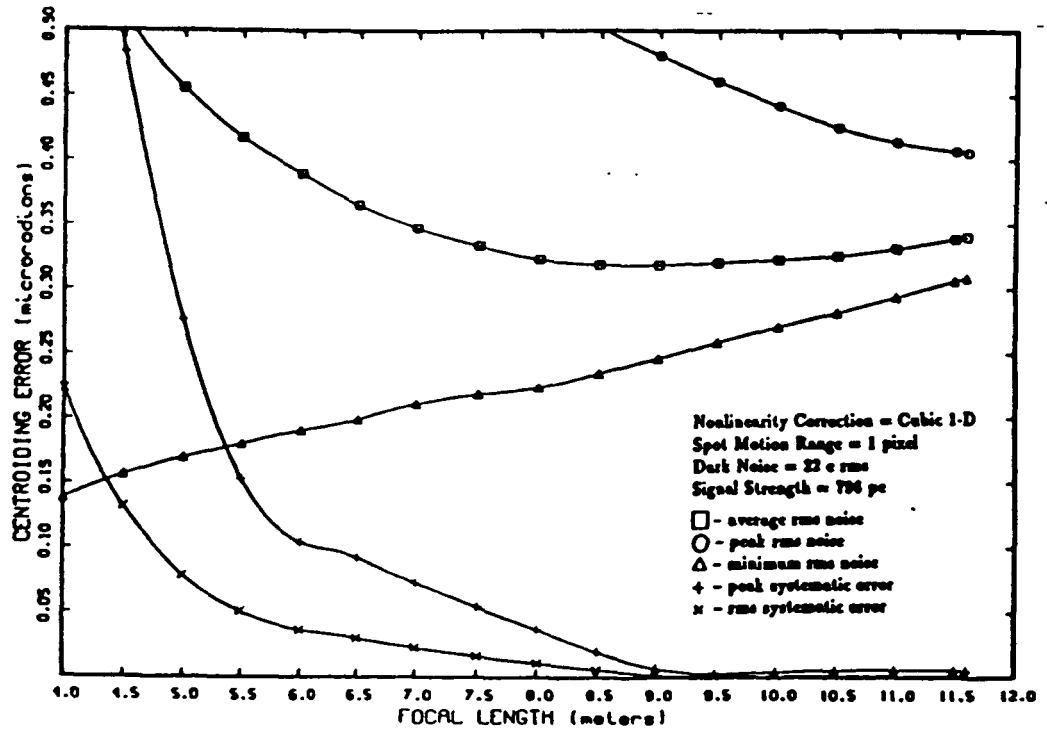

Figure 2: Systematic tracking error and tracking noise as a function of effective focal length.

the discrete sampling of the image PSF, background subtraction, and the necessary truncation of the image by the tracking algorithm. This results in a nonlinear relationship between the computed centroid and the actual centroid (the transfer function) which depends on the background noise and the size of the image relative to the sample size (i.e. the pixel size) and the number of pixels included in the centroiding algorithm. The algorithm also determines complexity of the signal processing electronics. The interaction of these factors complicates the selection of an optimum algorithm.

An optimised algorithm has been developed that implements a matched filter with parameters that are adjusted to minimise rms centroid noise equivalent displacement (NED), systematic (or bias) error, and rms signal strength estimation error. The optimised parameters in the matched filter tracking algorithm depend on the size of the PSF, as well as signal and background noise strengths.

Figure 2 shows some of the results of an analysis to determine the optimum PSF size. The power in Figure 2 corresponds to about 0.12 pW on the detector and the detector parameters were based on the Kodak HS-40, which will be described later. The curves show residual systematic errors that remain after third order polynomial corrections have been made, and the minimum, average, and peak random errors. The minimum of the average rms cnetroiding noise occur for a PSF size of about 1.9 to 2.4 pixels, the peak rms centroiding noise occurs at a PSF size of about 3 pixels. Figure 2 shows that at those PSF sizes the residual systematic errors are negligible.

We have analysed the performance of the algorithms over a range of signals and backgrounds to determine the sensitivity of the algorithm to the details of the optimization assumptions. Some of the results are shown in Figure 3. We have adopted a definition of the SNR designed to simplify the tradeoff between received beacon energy per frame and the system dark noise. The signal is defined as the total number of photoelectrons per frame generated in the focal plane by the beacon image regardless of the number of pixels covered. This value is a function of the beacon power, the frame rate, and the quantum efficiency. The array fill factor is assumed to be 1.0. The noise value is the noise in electrons for a single pixel in the absence of the beacon signal. This noise is composed of the intrinsic noise on a single pixel (including the processing electronics not present on the chip), the noise from the dark current, and the noise from the background photoelectrons. An alternative often used definition of SNR would also include the shot noise from the beacon and would sum the noise from all the pixels in the tracking window. Since the amount of energy captured by the pixels varies with spot position, and since the matched filter weights assigned to the pixels are not uniform, this would make it more difficult to interpret the results.

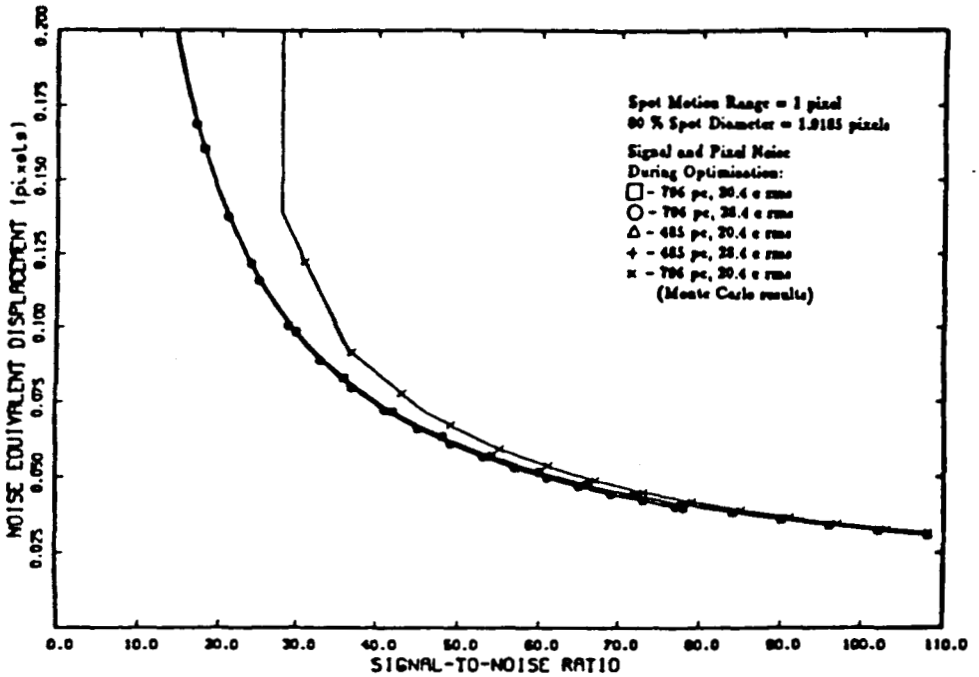

Figure 3: Average NED as a function of SNR, using a single set of optimised pixel weights. The analytic results are represented by the smooth curves and the Monte Carlo results are given by the broken curves.

It is seen in Figure 3 that NED is approximately inversely proportional to the SNR and has a weak dependence on the signal and background used in the optimisation.

7 Sensor Evaluation Criteria

Simple criteria for evaluation of candidate detectors for tracking optical communications beacons can be derived. The NED is approximately inversely proportional to the SNR:

$$NED = \frac{A}{SNR} \tag{2}$$

where A is determined by the centroiding algorithm. The FOV of a single pixel is given by the FOV of the entire array divided by the number of pixels in one direction along the detector, N. The NEA is given by:

$$NEA = \left(\frac{FOV}{N}\right) NED \tag{3}$$

so that:

$$NEA = A\left(\frac{FOV}{N}\right)\left(\frac{n}{S}\right) \tag{4}$$

where n is the noise in a single pixel and S is the total signal in the PSF. The signal can be written:

$$S = \eta\epsilon S_0 \tag{5}$$

where,

η is the quantum efficiency.
ϵ is the fill factor.
S_0 is the signal with quantum efficiency and fill factor of 100%.

If we collect all the sensor parameters onto one side of the equation and use the specification for the NEA, we can derive the following criteria for the sensor parameters:

$$\eta\epsilon\left(\frac{N}{n}\right) \geq A\left(\frac{FOV}{NEA}\right)\left(\frac{1}{S_{0,min}}\right) \tag{6}$$

where $S_{0,min}$ is the minimum signal that must meet the NEA specification. This result shows the proportionality between the sensor noise and the number of pixels required.

We find that for optimised algorithms $A \approx 2.3 - 4.0$. The value of S_{min} is computed to be 4330 photons per pW per

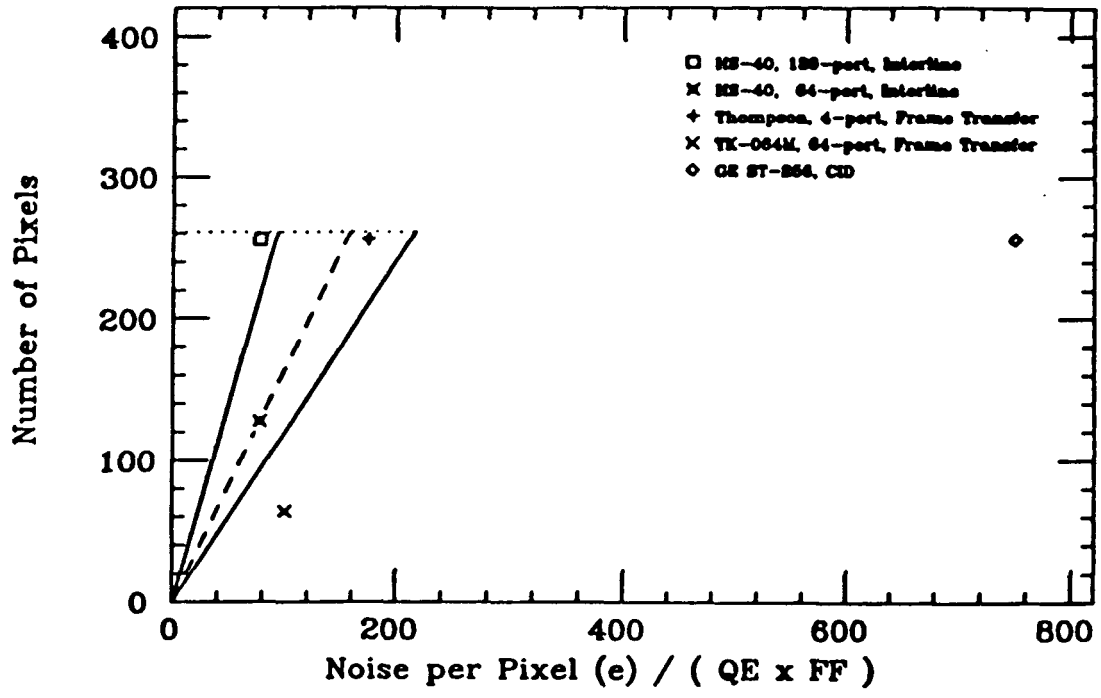

Figure 4: Sensor evaluation criteria and comparison of candidate detectors. The solid lines show the acceptable region as defined by equation 7. The dotted line show the criteria of equation 9. The update rate is 1000 Hs.

frame at 1000 frames/sec. If we set $FOV = 1000$ μrad and $NEA = 0.5$ μrad, which are the desired system specifications, we find:

$$\eta\epsilon\left(\frac{N}{n}\right) \geq \frac{B}{P_B} \tag{7}$$

where P_B is the received beacon power in picowatts. The values of B in picowatts are $\approx 1.0 - 1.8$. This result implies that for a sensor with $N = 256$, $\eta\epsilon = 0.3$, and $P_B = 0.43$ pW, the noise must be $n \leq 18$ to 33e, depending on the algorithm and tracking criteria.

Another sensor criterion can be obtained from the requirement to establish an optimum PSF size. The optimum PSF diameter is about two pixels across, which can be seen in the data presented in Figure 2. The optimum PSF diameter is not extremely sensitive. It is also desirable for the PSF to be established by the focus of diffraction limited optics. If the diffraction limited PSF is too small, either the image must be defocussed or aberrating elements must be introduced to expand the PSF. This is an undesirable method for establishing the PSF size due to difficulty in maintaining the PSF size and scale factor as a function of field angle.

Establishing the optimum PSF diameter on the sensor implies that two times the FOV of a single pixel, FOV/N, should be approximately equal to the 70% of the diffraction limited angle for the telescope, $2.44\lambda/D$. This condition puts limits on the number pixels in the sensor:

$$N \leq 2\left(\frac{FOV}{0.7\theta_{DL}}\right) \tag{8}$$

$$N \leq 263\left(\frac{D(cm)}{20}\right) . \tag{9}$$

We see that this condition requires that the number of pixels on the sensor be near (but less than) 263 for a 20 cm diameter telescope. This condition is much less critical than the limit on noise and number of pixels across the FOV.

7.1 Comparison of Sensors with Evaluation Criteria

We have examined all array detectors available today and have attempted to get information on detectors in development that may meet the criteria. Figure 4 shows how the best candidates compare in terms of the evaluation criteria derived in Section 7. The solid lines show the criteria of equation 7 for beacon powers of 0.4 and 1.0 pW and an update rate of 1000 Hs. The value of B in equation 7 was 1.2.

Kodak HS-40 Array	
Maximum Frame Rate	40,000 Hz
Pixel Spacing	32 by 32 μ m
Sensitive Area	24.2 by 30 μ m (71%)
Number of Pixels	128 by 128
Quantum Efficiency	0.43 @ 0.86 μ m
Dark Noise	20.4e rms @ 1000 Hz
Operating Temperature	20 deg C
Dark Current	2 na/cm^2
Charge Readout	Interline CCD
Output Channels	64 (128)
Pixel Rate Per Channel	10 (20) MHz
	0.512 @ 1000 Hz
Dark Current Variation	$\leq$5% rms
Responsivity Variation	5 % rms

Table 3: Performance Specifications for Kodak HS-40

The projected performance of the 128 port, 256x256 pixel HS-40 and the 4 port Thompson device meet the criteria for 1 pW of received power, but neither device is currently available. The only detector available today that can meet the specifications at 1.0 pW or less is the 128x128 HS-40. It specifications equals the evaluation criteria of equation 7 at a power of 0.62 pW, as shown by the dashed line on Figure 4.

7.2 Kodak HS-40

The Kodak HS40 is an interline transfer photodiode array that has been specially designed for high speed low noise applications. There are a number of innovations in the design to achieve the exceptional performance listed in table 3. Figure 5 shows the readout architecture of the device and Figure 6 shows the device that is currently being used in the POCAAD system.

Pinned Photodiodes

Photodiodes typically suffer from moderate to severe image lag. Image lag is an effect due to incomplete readout of the image charge so that some of the image charge remains and is readout in subsequent frames. This can be a severe effect at high frame rates. The lag results from the non-ideal nature of the MOSFET switch that gates the charge from the photodiode to the CCD shift register. When the photodiode is reset by moving the signal charge across the MOS transfer gate to the CCD, a thermionic emission-over-the-barrier process is responsible to removing the last of the charge. During the final stages of charge transfer the signal current drops exponentially. The final charge depends on the initial charge and the time interval. If the time interval is short, as in fast frame applications,

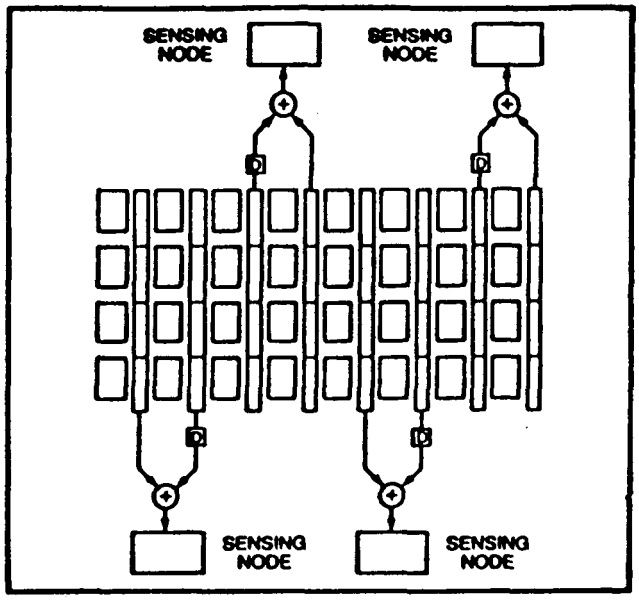

Figure 5: HS-40 readout architecture.

the reset charge is variable. The HS-40 has a more complex diode structure, the "pinned photodiode" [1], which has a complex doping profile that produces a potential gradient to push the charge out of the diode and allows complete removal of the signal charge. Using the pinned photodiode, the interline architecture can be used in high speed sensors at frame rates as high as 40,000 frames/sec with no significant image lag.

Shapped Potentials in CCD Shift Registers

The HS-40 uses an innovative design of the charge transfer wells in the interline CCD shift registers. The speed of the registers needed to be very fast (up to 10 MHz pixel rate) which is difficult to achieve in larger pixels due to the small field in the wells. The center of larger shift registers typically have very small transverse electric fields in the direction to push the charge along the shift register at high rates. The HS-40 design includes a tapered construction for the shift registers that creates an electric field that causes the shift registers to move charge at the 10 MHz rate with excellent charge transfer efficiency.

Metal Clock Lines

The clock lines on the HS-40 are metal lines, not polysilicon. Consequently they have lower resistance and dissipate less energy. This permits speed up of the clock lines. Metal lines can be used since they are routed over the CCD shift registers and act as the opaque light shields.

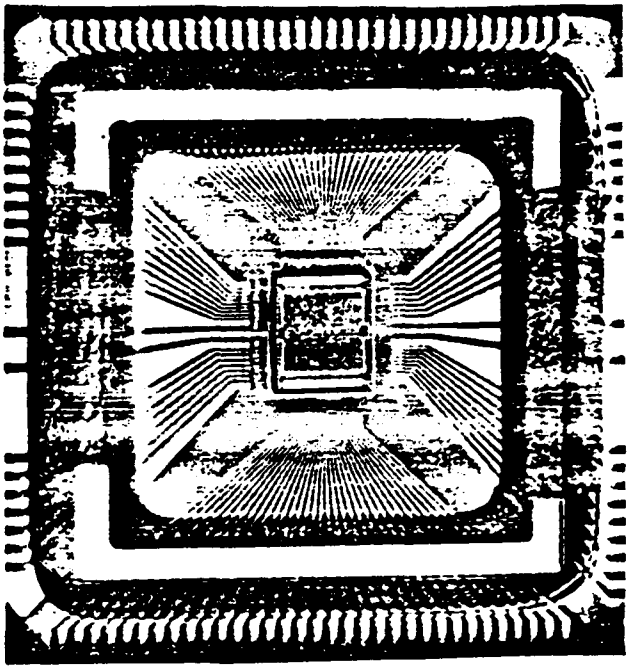

Figure 6: The HS-40 detector currently being used in test of the POCAAD system. 32 readout ports are on the top and bottom of the detector and clock signals are on the sides.

Parallelism of the Readout Architecture

The HS-40 has two columns per output port so that the data rate in each channel is lower and charge transfer rates and clock frequencies are kept to a minimum. This is essential for very low noise systems.

High Fill Factor - Quantum Efficiency Product

The fill factor of the HS-40 is unusually large for an interline device (72%). The quantum efficiency is also high since the device uses photodiodes.

Efficient Movement of Small Charge Packets

Difficulties of charge transfer efficiency and charge loss are also crucial considerations that are difficult to anticipate. In beacon acquisition and tracking the signals are only a few hundred electrons per pixel. Many sensors with excellent performance lose small amounts of charge in wells and traps that act as recombination centers. Loss of a few electrons is of importance in only the most demanding applications. Early HS-40 devices experienced loss of up to 800 electrons per pixels due to a very subtle "charge pumping" effect. A very small mask misalignment created a region in which electrons and holes were alternately pumped. At high rates the relaxation time of the charges was not rapid enough and the site acted as a recombination center. This points out the fact that sensors that operate in a satisfactory way a low rate cannot always be successfully operated in configurations that require high speed clocking. This is a significant risk in the use sensors in Y windowing or XY windowing modes that involve very high speed transfer of the charge.

8 Proof-of-Concept System

The purpose of the POC system is to demonstrate that the critical parameters of an operational system can be met. For the optical communications beacon acquisition, tracking, and point ahead system the crucial issues are:

- Low noise operation of an area array sensor at update rates of 1000 to 5000 Hz.
- Tracking using an optimized tracking algorithm at the required rates.
- Ability to acquire target within the required 30 seconds with a high probability of acquisition and a low probability of false acquisition with realistic signal and background levels.
- Ability to track a target moving at rates characteristic of operational conditions.
- Precision tracking with NED small enough to demonstrate NEA of ≤ 0.5 μrad.
- Residual systematic displacement error equivalent to ≤ 0.25 μrad to demonstrate point ahead precision.

The demonstration system needs to simulate the conditions listed in table 1.

The proposed POCAAD system is shown in Figure 7. Those aspects of the system that are not considered critical to the demonstration have been replaced by standard components such as: (a) the system controller is a Sun computer system and (b) the sources are simulated by diode lasers on computer controlled translation stages. The critical components are the detector, the drive electronics, the buffer electronics, and the acquisition and tracking digital signal processing electronics which are on VME boards.

The camera head consists of a stack of five PC boards, the detector board, clock electronics board, and three buffer electronics boards (two for the beacon beam and one for the reference beam). The buffer electronics implements an XY windowing scheme that permits only the data from the sensor in an 8 pixel wide strip around the beacon to processed. This is implemented by a series of programmable analog multiplexors that select the data of interest. This is under the control of the system controller. The buffer

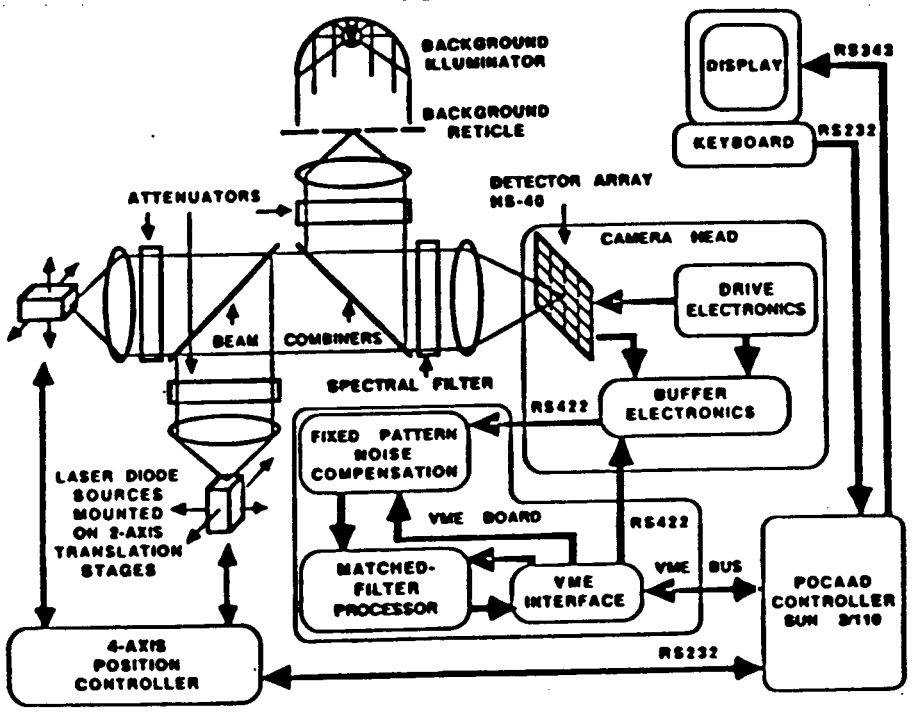

Figure 7: POCAAD System Layout.

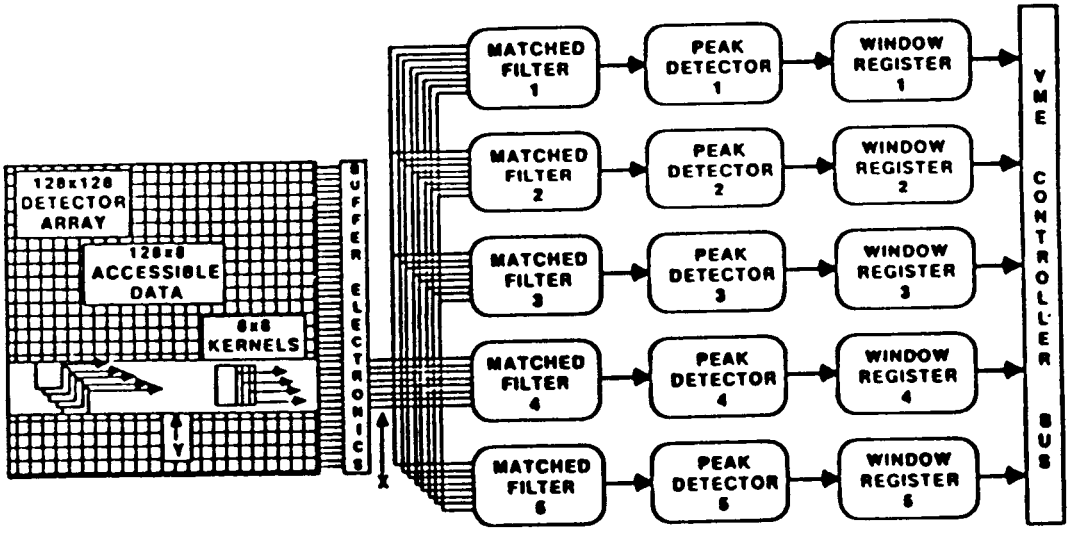

Figure 8: Acquisition Matched-Filter Implementation.

electronics determines the noise performance of the system. Digital signals are transmitted to the digital signal processing (DSP) board on the VME bus.

The DSP board plugs into a VME card cage, which is an extension of the Sun's bus. The data is corrected for the fixed pattern noise of the detector. This is essential when tracking to a small fraction of a pixel is required. The corrected data then is processed by a set of matched filters which can be used to implement acquisition or tracking algorithms. Figure 8 shows the arrangement of the matched filter processors when in the acquisition mode of operation. The system sweeps through the acquisition FOV in strips 8 pixels wide. Five filters operate on the data and implement 4x4 filters that are indexed across the strip. The output of each filter goes to a peak detector which stores the coordinates and signal strength of the pixel with the highest strength in the register. After 32 frames the entire FOV has been scanned and the registers contain the locations of the highest pixels. This entire process takes only 32 msec. The acquisition rate and false alarm rate have been discussed in a previous section.

When in the tracking mode the same filters, data comparitors, and registers are used to produce X and Y tracking error and normalisation energies, provide windowing of the data, and store the latest tracking data for access by the system controller. The controller has only to read the data, no calculations are required except to normalise the errors and determine if the X or Y widow coordinates need to be moved to remain centered on the beacon or reference.

This system is very flexible in that the operation of the filters, the sequence for reading and resetting the peak detectors, and the position of the data windows is determined by the system controller. The POC system can be used to evaluate several modes of operation and an operational system based on this architecture would be capable of several modes of operation and several algorithms for both acquisition and tracking could be implemented.

8.1 POC System Status

The analysis and design phases of the POC system are complete. The fabrication of the system is underway and the testing of the detector and electronics for the camera head is in progress. The entire system will be completed and under evaluation by the summer of 1989. Delivery to NASA laboratory at the Goddard Space Flight Center is scheduled for October 1989.

References

[1] B.C. Burkey, W.C. Chan, J. Littlehale, T.H. Lee, T.J. Tredwell, J.P. Lavine, E.A. Trabka, "The Pinned Photodiode for an Interline Transfer CCD image Sensor", Proceedings of the IEEE International Electron Devices Meeting, 28 (1984)